



**Queensland University of Technology**  
Brisbane Australia

This is the author's version of a work that was submitted/accepted for publication in the following source:

[Frost, Ray L.](#), [López, Andrés](#), [Xi, Yunfei](#), & [Scholz, Ricardo](#)  
(2014)

Vibrational spectroscopic characterization of the phosphate mineral althausite  $Mg_2(PO_4)(OH,F,O)$  – implications for the molecular structure.  
*Spectrochimica Acta Part A : Molecular and Biomolecular Spectroscopy*,  
120, pp. 252-256.

This file was downloaded from: <http://eprints.qut.edu.au/65137/>

© Copyright 2013 Elsevier B.V.

This is the author's version of a work that was accepted for publication in *Spectrochimica Acta Part A : Molecular and Biomolecular Spectroscopy*. Changes resulting from the publishing process, such as peer review, editing, corrections, structural formatting, and other quality control mechanisms may not be reflected in this document. Changes may have been made to this work since it was submitted for publication. A definitive version was subsequently published in *Spectrochimica Acta Part A : Molecular and Biomolecular Spectroscopy*, [VOL 120, (2014)] DOI: 10.1016/j.saa.2013.10.018

**Notice:** *Changes introduced as a result of publishing processes such as copy-editing and formatting may not be reflected in this document. For a definitive version of this work, please refer to the published source:*

<http://doi.org/10.1016/j.saa.2013.10.018>

1 **Vibrational spectroscopic characterization of the phosphate mineral althausite**  
2 **Mg<sub>2</sub>(PO<sub>4</sub>)(OH,F,O) – implications for the molecular structure**

3  
4  
5 **Ray L. Frost<sup>a\*</sup>, Andrés López<sup>a</sup>, Yunfei Xi<sup>a</sup>, Ricardo Scholz<sup>b</sup>**

6  
7 <sup>a</sup> School of Chemistry, Physics and Mechanical Engineering, Science and Engineering  
8 Faculty, Queensland University of Technology, GPO Box 2434, Brisbane Queensland 4001,  
9 Australia.

10  
11 <sup>b</sup> Geology Department, School of Mines, Federal University of Ouro Preto, Campus Morro do  
12 Cruzeiro, Ouro Preto, MG, 35,400-00, Brazil

13  
14 **Abstract:**

15 Natural single-crystal specimens of althausite from Brazil, with general formula  
16 Mg<sub>2</sub>(PO<sub>4</sub>)(OH,F,O) were investigated by Raman and infrared spectroscopy. The mineral  
17 occurs as a secondary product in granitic pegmatites. The Raman spectrum of althausite is  
18 characterized by bands at 1020, 1033 and 1044 cm<sup>-1</sup>, assigned to ν<sub>1</sub> symmetric stretching  
19 modes of the HOPO<sub>3</sub><sup>3-</sup> and PO<sub>4</sub><sup>3-</sup> units. Raman bands at around 1067, 1083 and 1138 cm<sup>-1</sup> are  
20 attributed to both the HOP and PO antisymmetric stretching vibrations. The set of Raman  
21 bands observed at 575, 589 and 606 cm<sup>-1</sup> are assigned to the ν<sub>4</sub> out of plane bending modes of  
22 the PO<sub>4</sub> and H<sub>2</sub>PO<sub>4</sub> units. Raman bands at 439, 461, 475 and 503 cm<sup>-1</sup> are attributed to the ν<sub>2</sub>  
23 PO<sub>4</sub> and H<sub>2</sub>PO<sub>4</sub> bending modes. Strong Raman bands observed at 312, 346 cm<sup>-1</sup> with  
24 shoulder bands at 361, 381 and 398 cm<sup>-1</sup> are assigned to MgO stretching vibrations. No  
25 bands which are attributable to water were found. Vibrational spectroscopy enables aspects of  
26 the molecular structure of althausite to be assessed.

27  
28 **Keywords:** althausite, phosphate, Raman, infrared, pegmatite

29  
30  

---

\* Author to whom correspondence should be addressed ([r.frost@qut.edu.au](mailto:r.frost@qut.edu.au))  
P +61 7 3138 2407 F: +61 7 3138 1804

31 1. **Introduction**

32 Althausite  $\text{Mg}_2(\text{PO}_4)(\text{OH},\text{F},\text{O})$  is a hydroxy phosphate of magnesium. The mineral is found in  
33 complex granitic pegmatites, formed by oxidation and hydration of primary minerals. The  
34 mineral originates from Minas Gerais [1], at the Sapucaia pegmatite mine, about 50 km east-  
35 southeast of Governador Valdares, and in good crystals from the Criminoso pegmatite mine,  
36 about 35 km north. The mineral varies in colour from dark blue-green to black. The mineral  
37 is found at many sites worldwide [1-9] including at Olary, South Australia [9], and is found  
38 in magnetite-serpentinite deposits. The name of the mineral honors Professor Egon Althaus  
39 (1933– ), Karlsruhe University, Karlsruhe, Germany.

40

41 The mineral is orthorhombic [10], pseudotetragonal with point group:  $2/m$ . The cell data is  
42 *Space Group:  $P2_1/c$ , with  $a = 8.258$ ,  $b = 6.054$ ,  $c = 14.383$ ,  $\beta = 120.150$  and  $Z = 4$ .*

43 According to Roemming and Raade, magnesium atoms occur in both five- and six-fold  
44 coordination, and the coordination polyhedra are highly distorted [10]. The Mg octahedra  
45 form chains along D by edge-sharing. Hydroxyl and fluorine occur in a largely ordered  
46 distribution among two different structural sites and occupy alternating positions along  
47 'channels' parallel to D. The mineral is related to the mineral wagnerite  $\text{Mg}_2\text{PO}_4\text{F}$  [11-14].  
48 Wagnerite may be considered the fluorine end-member and althausite, the hydroxyl end  
49 member. Another mineral, which is chemically closely related to althausite, is holtedahlite  
50  $\text{Mg}_2\text{PO}_4\text{OH}$  [15]. Althausite has some formal structural features in common with the  
51 minerals libethenite-olivenite-adamite-eveite-andalusite, in that they contain similar cation  
52 polyhedra with 5- and 6-coordination and the same kind of edge-sharing octahedral chains  
53 [12, 16]. Complex phase relationships exist in the  $\text{MgO-P}_2\text{O}_5\text{-H}_2\text{O}$  system [11].

54

55 Raman spectroscopy has proven most useful for the study of mineral structures. The objective  
56 of this research is to report the Raman and infrared spectra of althausite and to relate the  
57 spectra to the molecular structure of the mineral. This is the first report of a systematic study  
58 of the mineral althausite from Brazil.

59

## 60 2. Experimental

### 61 2.1 Samples description and preparation

62 The althausite sample studied in this work was collected from Minas Gerais [1], at the  
63 Sapucaia pegmatite mine, about 50 km east-southeast of Governador Valdares. The sample  
64 was incorporated to the collection of the Geology Department of the Federal University of  
65 Ouro Preto, Minas Gerais, Brazil, with sample code SAC-024.

66

### 67 2.2 Scanning electron microscopy (SEM)

68 Experiments and analyses involving electron microscopy were performed in the Center of  
69 Microscopy of the Universidade Federal de Minas Gerais, Belo Horizonte, Minas Gerais,  
70 Brazil (<http://www.microscopia.ufmg.br>). Althausite crystal cleavage fragment was coated  
71 with a 5 nm layer of evaporated Au. Secondary Electron and Backscattering Electron images  
72 were obtained using a JEOL JSM-6360LV equipment.

73

### 74 2.3 Raman microprobe spectroscopy

75 Crystals of althausite were placed on a polished metal surface on the stage of an Olympus  
76 BHSM microscope, which is equipped with 10x, 20x, and 50x objectives. The microscope is  
77 part of a Renishaw 1000 Raman microscope system, which also includes a monochromator, a  
78 filter system and a CCD detector (1024 pixels). The Raman spectra were excited by a  
79 Spectra-Physics model 127 He-Ne laser producing highly polarized light at 633 nm and  
80 collected at a nominal resolution of  $2\text{ cm}^{-1}$  and a precision of  $\pm 1\text{ cm}^{-1}$  in the range between  
81 200 and  $4000\text{ cm}^{-1}$ . Repeated acquisitions on the crystals using the highest magnification  
82 (50x) were accumulated to improve the signal to noise ratio of the spectra. Raman Spectra  
83 were calibrated using the  $520.5\text{ cm}^{-1}$  line of a silicon wafer. The Raman spectrum of at least  
84 10 crystals was collected to ensure the consistency of the spectra.

85

### 86 2.4 Infrared spectroscopy

87 Infrared spectra were obtained using a Nicolet Nexus 870 FTIR spectrometer with a smart  
88 endurance single bounce diamond ATR cell. Spectra over the  $4000\text{--}525\text{ cm}^{-1}$  range were  
89 obtained by the co-addition of 128 scans with a resolution of  $4\text{ cm}^{-1}$  and a mirror velocity of  
90  $0.6329\text{ cm/s}$ . Spectra were co-added to improve the signal to noise ratio.

91

92 Spectral manipulation such as baseline correction/adjustment and smoothing were performed  
93 using the Spectralcalc software package GRAMS (Galactic Industries Corporation, NH,  
94 USA). Band component analysis was undertaken using the Jandel 'Peakfit' software package  
95 that enabled the type of fitting function to be selected and allows specific parameters to be  
96 fixed or varied accordingly. Band fitting was done using a Lorentzian-Gaussian cross-product  
97 function with the minimum number of component bands used for the fitting process. The  
98 Gaussian-Lorentzian ratio was maintained at values greater than 0.7 and fitting was  
99 undertaken until reproducible results were obtained with squared correlations of  $r^2$  greater  
100 than 0.995.

101

### 102 3. Results and discussion

103

#### 104 3.1 *Vibrational Spectroscopy Background*

105 In aqueous systems, the Raman spectra of phosphate oxyanions show a symmetric stretching  
106 mode ( $\nu_1$ ) at  $938\text{ cm}^{-1}$ , an antisymmetric stretching mode ( $\nu_3$ ) at  $1017\text{ cm}^{-1}$ , a symmetric  
107 bending mode ( $\nu_2$ ) at  $420\text{ cm}^{-1}$  and a  $\nu_4$  bending mode at  $567\text{ cm}^{-1}$  [17-19]. S.D. Ross in  
108 Farmer listed some well-known minerals containing phosphate which were either hydrated or  
109 hydroxylated or both [20]. The vibrational spectrum of the dihydrogen phosphate anion has  
110 been reported by Farmer [20]. The  $\text{PO}_2$  symmetric stretching mode occurs at  $1072\text{ cm}^{-1}$  and  
111 the POH symmetric stretching mode at  $\sim 878\text{ cm}^{-1}$ . The POH antisymmetric stretching mode  
112 was found at  $947\text{ cm}^{-1}$  and the  $\text{P}(\text{OH})_2$  bending mode at  $380\text{ cm}^{-1}$ . The band at  $1150\text{ cm}^{-1}$  was  
113 assigned to the  $\text{PO}_2$  antisymmetric stretching mode. The position of these bands will shift  
114 according to the crystal structure of the mineral.

115

116 The vibrational spectra of phosphate minerals have been published by Farmer's treatise  
117 Chapter 17 [20]. The Table 17.III in ref. [20] reports the band positions of a wide range of  
118 phosphates and arsenates. The band positions for the monohydrogen phosphate anion of  
119 disodium hydrogen phosphate dihydrate is given as  $\nu_1$  at  $820$  and  $866\text{ cm}^{-1}$ ,  $\nu_2$  at around  $460$   
120  $\text{cm}^{-1}$ ,  $\nu_3$  as  $953, 993, 1055, 1070, 1120$  and  $1135\text{ cm}^{-1}$ ,  $\nu_4$  at  $520, 539, 558, 575\text{ cm}^{-1}$ . The  
121 POH unit has vibrations associated with the OH specie. The stretching vibration of the POH  
122 units was tabulated as  $2430$  and  $2870\text{ cm}^{-1}$ , and bending modes at  $766$  and  $1256\text{ cm}^{-1}$ . Water  
123 stretching vibrations were found at  $3050$  and  $3350\text{ cm}^{-1}$ . The position of the bands for the  
124 disodium hydrogen phosphate is very dependent on the waters of hydration. There have been

125 several Raman spectroscopic studies of the monosodium dihydrogen phosphate chemicals  
126 [21-25].

127

### 128 **3.2 Vibrational Spectroscopy**

129 The Raman spectrum of althausite over the 100 to 4000  $\text{cm}^{-1}$  spectral range is illustrated in  
130 **Figure 1a**. This figure shows the peak position and the relative intensities of the Raman  
131 bands. It is noted there are large parts of the spectrum where no intensity is observed and  
132 therefore, the spectrum is subdivided into sections based upon the types of vibration being  
133 studied. The infrared spectrum of althausite over the 500 to 4000  $\text{cm}^{-1}$  spectral range is  
134 reported in **Figure 1b**. This figure shows the position and relative intensities of the infrared  
135 bands. There are large parts of the infrared spectrum where little or no intensity is observed.  
136 Hence, the spectrum is subdivided into sections based on which bands are being studied.

137

138 The Raman spectrum of althausite over the 800 to 1200  $\text{cm}^{-1}$  spectral range are reported in  
139 **Figure 2a**. The Raman spectrum of althausite in this spectral region shows complexity with a  
140 series of overlapping bands. The chemistry of althausite is such that it is expected to have  
141 interactions between the phosphate and hydroxyl units. This means that  $\text{HOPO}_3^{3-}$  units will  
142 form. Raman bands are observed at 964, 986 and 993  $\text{cm}^{-1}$ . It is proposed that these three  
143 bands are attributed to the PO stretching vibrations of  $\text{HOPO}_3^{3-}$ ,  $\text{PO}_4^{3-}$  and  $\text{H}_2\text{PO}_4^-$  units.  
144 According to Roemming and Raade [10], the phosphate units in the crystal structure of  
145 althausite are not equivalent and the interaction with the hydroxyl or fluorine units will be  
146 different, so it is not unexpected that a number of phosphate stretching vibrations would be  
147 observed.

148

149

150 Galy [23] first studied the polarized Raman spectra of the  $\text{H}_2\text{PO}_4^-$  anion. Choi *et al.* reported  
151 the polarization spectra of  $\text{NaH}_2\text{PO}_4$  crystals. Casciani and Condrate [26] published spectra  
152 on brushite and monetite together with synthetic anhydrous monocalcium phosphate  
153 ( $\text{Ca}(\text{H}_2\text{PO}_4)_2$ ), monocalcium dihydrogen phosphate hydrate ( $\text{Ca}(\text{H}_2\text{PO}_4)_2 \cdot \text{H}_2\text{O}$ ) and  
154 octacalcium phosphate ( $\text{Ca}_8\text{H}_2(\text{PO}_4)_6 \cdot 5\text{H}_2\text{O}$ ). These authors determined band assignments for  
155  $\text{Ca}(\text{H}_2\text{PO}_4)_2$  and reported bands at 1012 and 1085  $\text{cm}^{-1}$  as POH and PO stretching vibrations,  
156 respectively. The three Raman bands at 1033, 1049 and 1062  $\text{cm}^{-1}$  are attributed to both the  
157 HOP and PO antisymmetric stretching vibrations. Casciani and Condrate [26] tabulated  
158 Raman bands at 1132 and 1155  $\text{cm}^{-1}$  and assigned these bands to P-O symmetric and the P-O

159 antisymmetric stretching vibrations. It is proposed that the proton on the hydroxyl units is  
160 very liable and can oscillate between the OH units and the phosphate units. In this way the  
161 hydrogen phosphate units are formed. The low intensity Raman bands at 968 and 988  $\text{cm}^{-1}$   
162 are ascribed to the hydroxyl deformation modes of the OH units in the althausite structure.

163

164 The infrared spectrum of althausite is shown in [Figure 2b](#). This infrared spectrum shows even  
165 greater complexity than the Raman spectrum ([Figure 2a](#)). The infrared spectrum may be band  
166 component analyzed into component bands. The infrared bands at 932, 976 and 1002  $\text{cm}^{-1}$   
167 are assigned to the PO stretching vibrations of the  $\text{HOPO}_3^{3-}$ ,  $\text{PO}_4^{3-}$  and  $\text{H}_2\text{PO}_4^-$  units. The  
168 three infrared bands at 1031, 1066 and 1135  $\text{cm}^{-1}$  are assigned to the antisymmetric stretching  
169 vibrations of these units.

170

171 The Raman spectra of althausite in the 400 to 700  $\text{cm}^{-1}$  and 100 to 400  $\text{cm}^{-1}$  spectral range are  
172 displayed in [Figure 3](#). The spectrum in [Figure 3a](#) may be subdivided into sections. (a) the  
173 bands at around 589  $\text{cm}^{-1}$  (b) the bands in the 439 to 503  $\text{cm}^{-1}$  spectral range and (c) bands in  
174 the 312 to 398  $\text{cm}^{-1}$ . In addition, there is a low intensity band at 702  $\text{cm}^{-1}$ . The Raman bands  
175 observed at 575, 589 and 606  $\text{cm}^{-1}$  are assigned to the  $\nu_4$  out of plane bending modes of the  
176  $\text{PO}_4$  and  $\text{H}_2\text{PO}_4$  units. The Raman spectrum of  $\text{NaH}_2\text{PO}_4$  shows bands at 526, 546 and 618  
177  $\text{cm}^{-1}$ . The observation of multiple bands in this spectral region supports the concept of  
178 symmetry reduction of both the phosphate and hydrogen phosphate units. Raman bands at  
179 439, 461, 475 and 503  $\text{cm}^{-1}$  are attributed to the  $\nu_2$   $\text{PO}_4$  and  $\text{H}_2\text{PO}_4$  bending modes. The  
180 Raman spectrum of  $\text{NaH}_2\text{PO}_4$  shows two Raman bands at 460 and 482  $\text{cm}^{-1}$ . The observation  
181 of multiple Raman bands in this spectral region for the althausite mineral supports the  
182 concept of symmetry reduction of the phosphate anion. Strong Raman bands are observed at  
183 312, 346  $\text{cm}^{-1}$  with shoulder bands at 361, 381 and 398  $\text{cm}^{-1}$ . These bands are assigned to  
184 MgO stretching vibrations. Again, the observation of multiple bands in this spectral region  
185 supports the concept of the non-equivalence of phosphate units in the structure of althausite.  
186 There are a number of bands in the Raman spectrum of the far low wavenumber region.  
187 These bands are ascribed to lattice vibrations.

188

189 The Raman spectrum in the 3300 to 3800  $\text{cm}^{-1}$  spectral region is displayed in [Figure 4a](#). The  
190 spectral profile is complex with multiple overlapping bands. Raman bands are observed at  
191 3472, 3488, 3500, 3511 and 3523  $\text{cm}^{-1}$ . These bands are assigned to the OH stretching  
192 vibrations of the OH units in the althausite structure. From these values, a hydrogen bond

193 distance may be calculated of around 2.94 Å, which is in good agreement with that obtained  
194 from XRD data of 2.39 Å [10]. The Raman spectrum over the 1100 to 1400 cm<sup>-1</sup> spectral  
195 range is shown in Figure 5a. No Raman bands at around 1630 cm<sup>-1</sup> were observed, thus  
196 confirming the absence of water in the structure of althausite. A broad Raman peak was  
197 found at around 1320 cm<sup>-1</sup> and a sharper peak at 1130 cm<sup>-1</sup> was observed.

198

199 The infrared spectrum of althausite in the 2800 to 3800 cm<sup>-1</sup> spectral range is reported in  
200 Figure 4b. The spectrum is broad with the main peak observed at 3500 cm<sup>-1</sup>. There is a long  
201 tail on the low wavenumber side and additional bands may be resolved. These bands may be  
202 attributed to the stretching vibrations of the OH units. An additional infrared band at 3679  
203 cm<sup>-1</sup> is observed. The infrared spectrum of althausite showed no bands at around 1630 cm<sup>-1</sup>.  
204 This indicates that no water was present (Figure 5b). Raade and Tysseland reported the  
205 infrared spectrum of althausite in their paper of 1975. They showed a stretching wavenumber  
206 for althausite at 3510 cm<sup>-1</sup> [27]. These workers also synthesised the mineral analogue of  
207 althausite for which some splitting of the infrared bands occurred' thus indicating the non-  
208 equivalence of the OH units in the structure of althausite. Such a concept is strongly  
209 supported by our Raman spectra where multiple OH stretching vibrations are observed.

210

#### 211 4. Conclusions

212 Althausite is one of many phosphate minerals found in granitic pegmatites. However, this  
213 particular phosphate mineral of formula Mg<sub>2</sub>(PO<sub>4</sub>)(OH,F,O) is an anhydrous mineral in which  
214 no water is present in the mineral formula. Whilst the colour of the mineral varies and is  
215 probably a function of the mineral origin, the mineral is often black or bluish black. Thus, it  
216 might be expected that the mineral might be difficult to measure its Raman spectrum; however  
217 this is not the case and the Raman spectra are readily obtained.

218

219 The mineral is a typical phosphate and Raman and infrared bands are attributed to HOP and  
220 PO bending and stretching vibrations of the HOPO<sub>3</sub><sup>3-</sup> and PO<sub>4</sub><sup>3-</sup> units. The Raman spectrum  
221 of althausite shows multiple bands attributable to the OH units. At least four bands are  
222 observed, thus indicating the non-equivalence of the OH units in the althausite structure. The  
223 infrared spectrum displays a broad band centred upon 3500 cm<sup>-1</sup>. Vibrational spectroscopy  
224 enables aspects of the molecular structure of althausite to be assessed.

225



226

227

228 **Acknowledgments**

229 The financial and infra-structure support of the Discipline of Nanotechnology and Molecular  
230 Science, Science and Engineering Faculty of the Queensland University of Technology, is  
231 gratefully acknowledged. The Australian Research Council (ARC) is thanked for funding the  
232 instrumentation. The authors would like to acknowledge the Center of Microscopy at the  
233 Universidade Federal de Minas Gerais (<http://www.microscopia.ufmg.br>) for providing the  
234 equipment and technical support for experiments involving electron microscopy. R. Scholz  
235 thanks to CNPq – Conselho Nacional de Desenvolvimento Científico e Tecnológico (grant  
236 No. 306287/2012-9).

237

238

239 **References**

240

- 241 [1] M. Bajjot, F. Hatert, S. Philippo, Mineralogy and geochemistry of phosphates and  
242 silicates in the Sapucaia pegmatite, Minas Gerais, Brazil: genetic implications, *Canadian*  
243 *Mineralogist*, 50 (2012) 1531-1554.
- 244 [2] T.J. Campbell, W.L. Roberts, Phosphate minerals from the Tip Top mine, Black Hills,  
245 South Dakota, *Mineralogical Record*, 17 (1986) 237-254.
- 246 [3] F. Cech, Z. Johan, P. Povondra, Barbosalite of the South Angarf pegmatite, Tazenakht  
247 Plain, Anti-Atlas, Morocco, *Notes et Memoires du Service Geologiques (Morocco)*, 32  
248 (1972) 121-128.
- 249 [4] A.M. Fransolet, Lithium-bearing phosphates of the pegmatites of the Zenaya Plain, Anti-  
250 Atlas, Morocco, *Notes et Memoires du Service Geologiques (Morocco)*, 35 (1974) 137-143.
- 251 [5] J.d.R. Hirson, The phosphates of Sapucaia, *Anais da Academia Brasileira de Ciencias*, 37  
252 (1965) 471-475.
- 253 [6] P. Keller, Phosphate minerals from pegmatites of South West Africa, *Aufschluss*, 25  
254 (1974) 577-591.
- 255 [7] P. Keller, Giniite,  $\text{Fe}_2+\text{Fe}_{43+}[(\text{H}_2\text{O})_2(\text{OH})_2(\text{PO}_4)_4]$ , a new mineral from the pegmatite  
256 of Sandamab near Usakos, Namibia, *Neues Jahrbuch fuer Mineralogie, Monatshefte*, (1980)  
257 49-56.
- 258 [8] P.B. Leavens, T.A. Simpson, Iron-manganese phosphates of the Williams pegmatites,  
259 Coosa County, Alabama, *Mineralogical Record*, 6 (1975) 64-73.
- 260 [9] I.R. Plimer, I.D. Blucher, Wolfeite and barbosalite from Thackaringa, Australia, *Mineral.*  
261 *Mag.*, 43 (1979) 505-507.
- 262 [10] C. Roemming, G. Raade, The crystal structure of althausite,  $\text{Mg}_4(\text{PO}_4)_2(\text{OH},\text{O})(\text{F},\square)$ ,  
263 *American Mineralogist*, 65 (1980) 488-498.
- 264 [11] F. Brunet, C. Chopin, F. Seifert, Phase relations in the MgO-P<sub>2</sub>O<sub>5</sub>-H<sub>2</sub>O system and the  
265 stability of phosphoellenbergerite: petrological implications, *Contributions to Mineralogy and*  
266 *Petrology*, 131 (1998) 54-70.
- 267 [12] G. Raade, Hydrothermal syntheses of Mg<sub>2</sub>PO<sub>4</sub>OH polymorphs, *Neues Jahrbuch fuer*  
268 *Mineralogie, Monatshefte*, (1990) 289-300.
- 269 [13] A. Coda, G. Giuseppetti, C. Tadini, The crystal structure of wagnerite, *Atti della*  
270 *Accademia Nazionale dei Lincei, Classe di Scienze Fisiche, Matematiche e Naturali,*  
271 *Rendiconti*, 43 (1967) 212-224.
- 272 [14] L. Ren, E.S. Grew, M. Xiong, Z. Ma, Wagnerite-Ma5bc, a new polytype of  
273  $\text{Mg}_2(\text{PO}_4)(\text{F},\text{OH})$ , from granulite-facies paragneiss, Larsemann Hills, Prydz Bay, East  
274 Antarctica, *Canadian Mineralogist*, 41 (2003) 393-411.
- 275 [15] G. Raade, M.H. Mladeck, Høltedahlite, a new magnesium phosphate from Modum,  
276 Norway, *Lithos*, 12 (1979) 283-287.
- 277 [16] G. Raade, C. Roemming, The crystal structure of β-magnesium hydroxide phosphate  
278 ( $\text{Mg}_2\text{PO}_4\text{OH}$ ), a synthetic hydroxyl analogue of wagnerite, *Zeitschrift fuer Kristallographie*,  
279 177 (1986) 15-26.
- 280 [17] R.L. Frost, W. Martens, P.A. Williams, J.T. Kloprogge, Raman and infrared  
281 spectroscopic study of the vivianite-group phosphates vivianite, baricite and bobierite,  
282 *Mineralogical Magazine*, 66 (2002) 1063-1073.
- 283 [18] R.L. Frost, W.N. Martens, T. Kloprogge, P.A. Williams, Vibrational spectroscopy of the  
284 basic manganese and ferric phosphate minerals: strunzite, ferrostrunzite and ferristrunzite,  
285 *Neues Jahrbuch fuer Mineralogie, Monatshefte*, (2002) 481-496.

- 286 [19] R.L. Frost, P.A. Williams, W. Martens, J.T. Kloprogge, P. Leverett, Raman  
287 spectroscopy of the basic copper phosphate minerals cornetite, libethenite, pseudomalachite,  
288 reichenbachite and ludjibaite, *Journal of Raman Spectroscopy*, 33 (2002) 260-263.
- 289 [20] V.C. Farmer, *Mineralogical Society Monograph 4: The Infrared Spectra of Minerals*,  
290 1974.
- 291 [21] C.E. Bamberger, W.R. Busing, G.M. Begun, R.G. Haire, L.C. Ellingboe, Raman  
292 spectroscopy of polymorphic orthophosphates containing sodium and lanthanide elements,  
293 *Journal of Solid State Chemistry*, 57 (1985) 248-259.
- 294 [22] B.K. Choi, M.N. Lee, J.J. Kim, Raman spectra of the sodium hydrogen phosphate  
295 ( $\text{NaH}_2\text{PO}_4$ ) crystal, *Journal of Raman Spectroscopy*, 20 (1989) 11-15.
- 296 [23] A. Galy, The Raman spectrum of a single crystal of  $\text{NaH}_2\text{PO}_4 \cdot 2\text{H}_2\text{O}$ , *Journal de*  
297 *Physique et le Radium*, 12 (1951) 827.
- 298 [24] H. Poulet, N. Toupry-Krauzman, Raman spectra of a single crystal of sodium  
299 dihydrogen phosphate dihydrate, *Proc. Int. Conf. Raman Spectrosc.*, 6th, 2 (1978) 364-365.
- 300 [25] N. Toupry-Krauzman, H. Poulet, M. Le Postollec, A Raman spectroscopic study of  
301 single crystals of sodium monobasic phosphate dihydrate and sodium monobasic phosphate-  
302  $\text{d}_2$  dihydrate- $\text{d}_2$ , *Journal of Raman Spectroscopy*, 8 (1979) 115-121.
- 303 [26] F.S. Casciani, R.A. Condrate, Sr., The infrared and Raman spectra of several calcium  
304 hydrogen phosphates, *Proceedings - International Congress on Phosphorus Compounds*, 2nd  
305 (1980) 175-190.
- 306 [27] G. Raade, M. Tysseland, Althausite, a new mineral from Modum, Norway, *Lithos*, 8  
307 (1975) 215-219.
- 308
- 309

310 **List of Figures**

311

312 **Figure 1 (a) Raman spectrum of althausite over the 100 to 4000  $\text{cm}^{-1}$  spectral range (b)**  
313 **Infrared spectrum of althausite over the 500 to 4000  $\text{cm}^{-1}$  spectral range**

314

315 **Figure 2 (a) Raman spectrum of althausite over the 800 to 1400  $\text{cm}^{-1}$  spectral range (b)**  
316 **Infrared spectrum of althausite over the 500 to 1300  $\text{cm}^{-1}$  spectral range**

317

318 **Figure 3 (a) Raman spectrum of althausite over the 400 to 700  $\text{cm}^{-1}$  spectral range (b)**  
319 **Raman spectrum of althausite over the 100 to 400  $\text{cm}^{-1}$  spectral range**

320

321 **Figure 4 (a) Raman spectrum of althausite over the 3300 to 3800  $\text{cm}^{-1}$  spectral range (b)**  
322 **Infrared spectrum of althausite over the 2800 to 3800  $\text{cm}^{-1}$  spectral range**

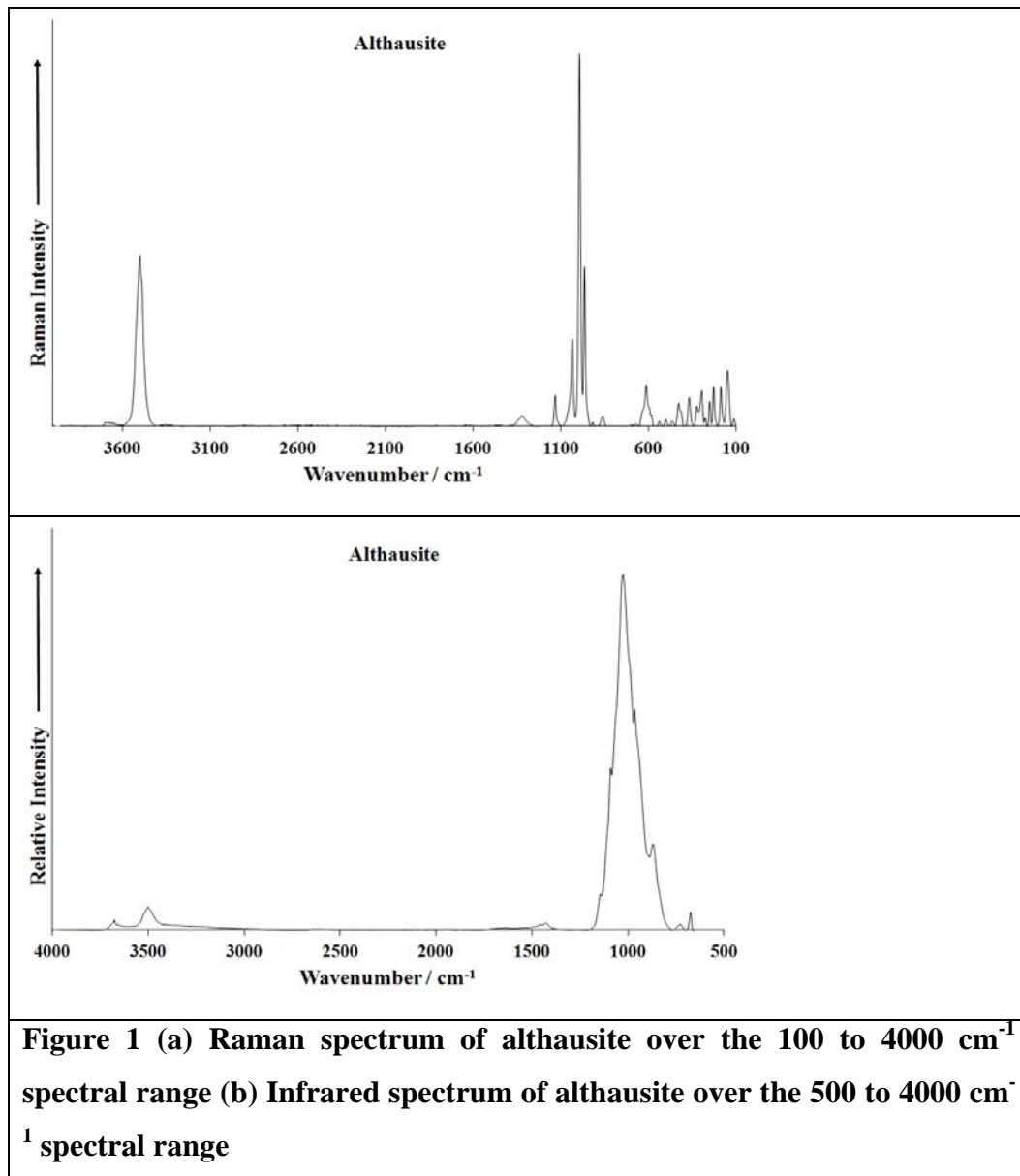
323

324 **Figure 5 (a) Raman spectrum of althausite (upper spectrum) in the 1100 to 1400  $\text{cm}^{-1}$**   
325 **spectral range (b) infrared spectrum of althausite (lower spectrum) in the 1300 to 1700**  
326  **$\text{cm}^{-1}$  spectral range**

327

328

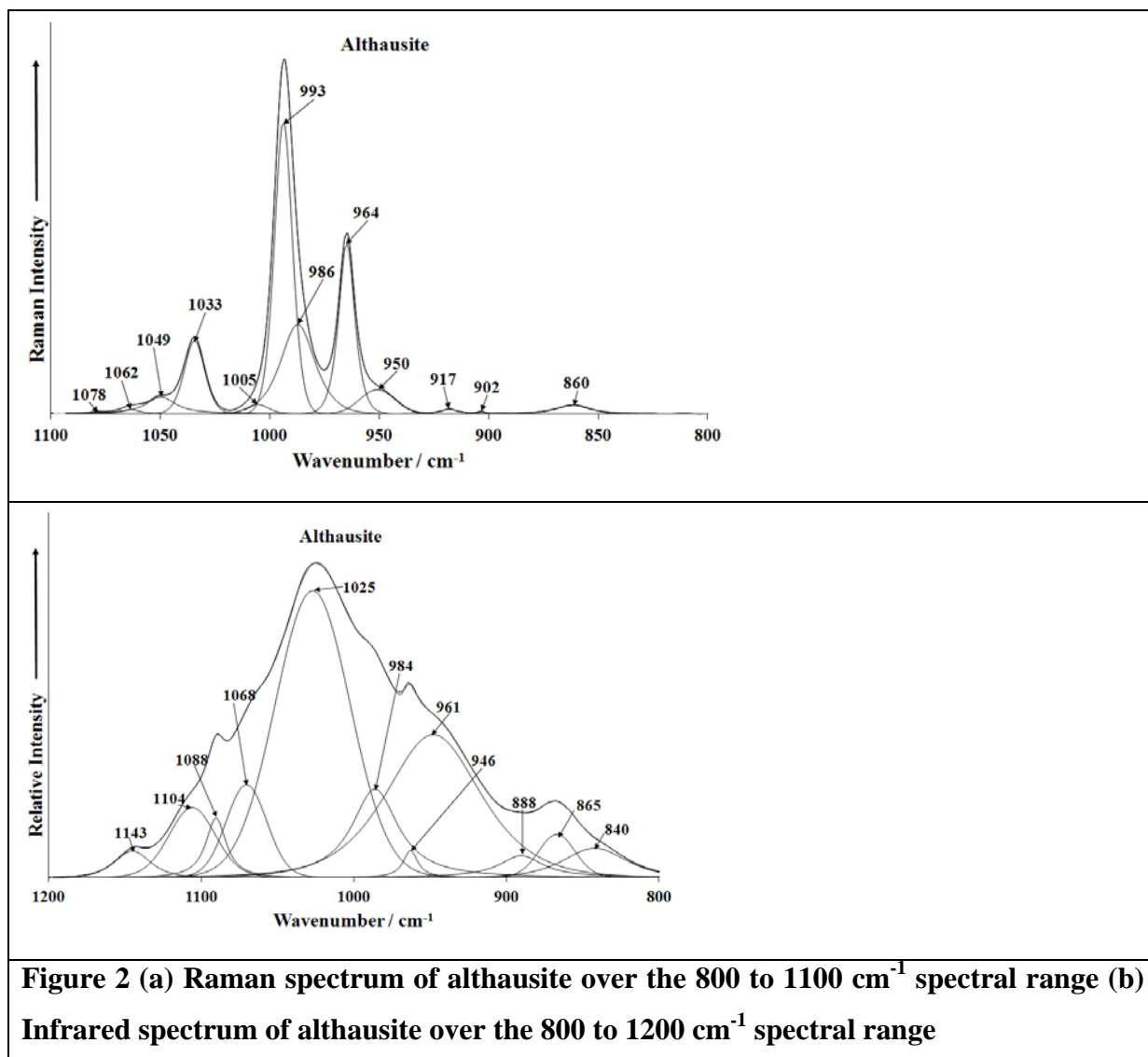
329

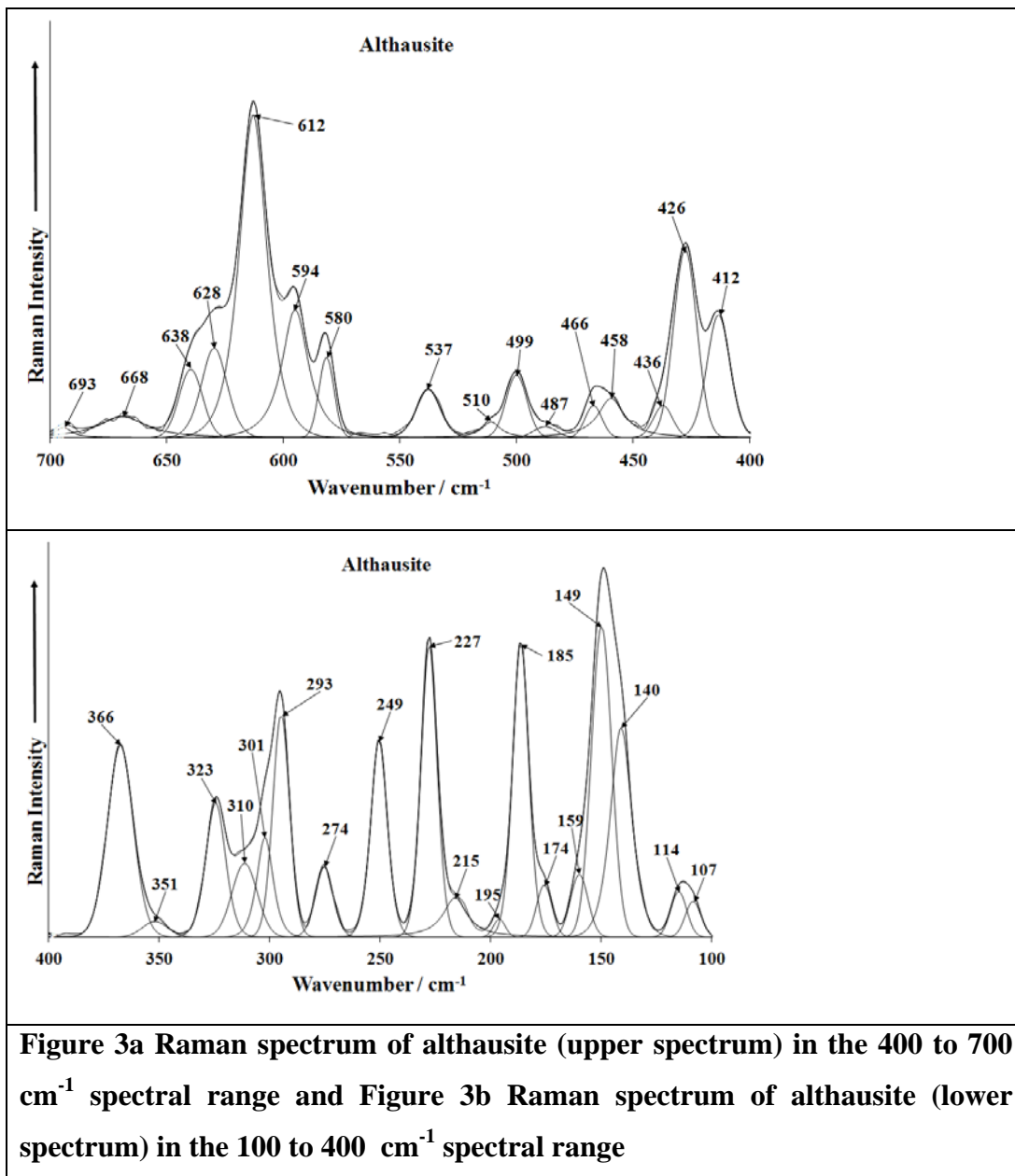


330

331

332





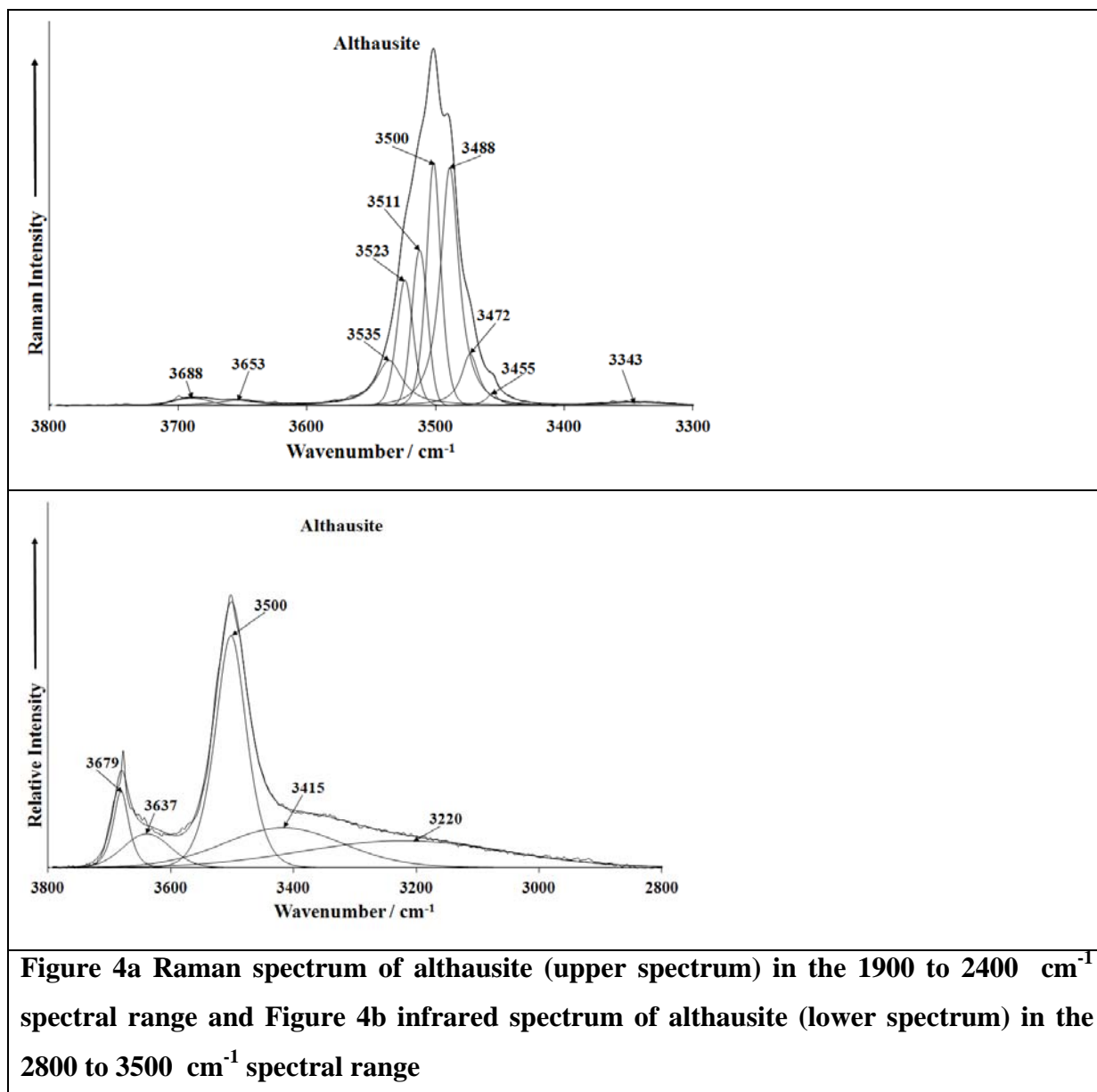
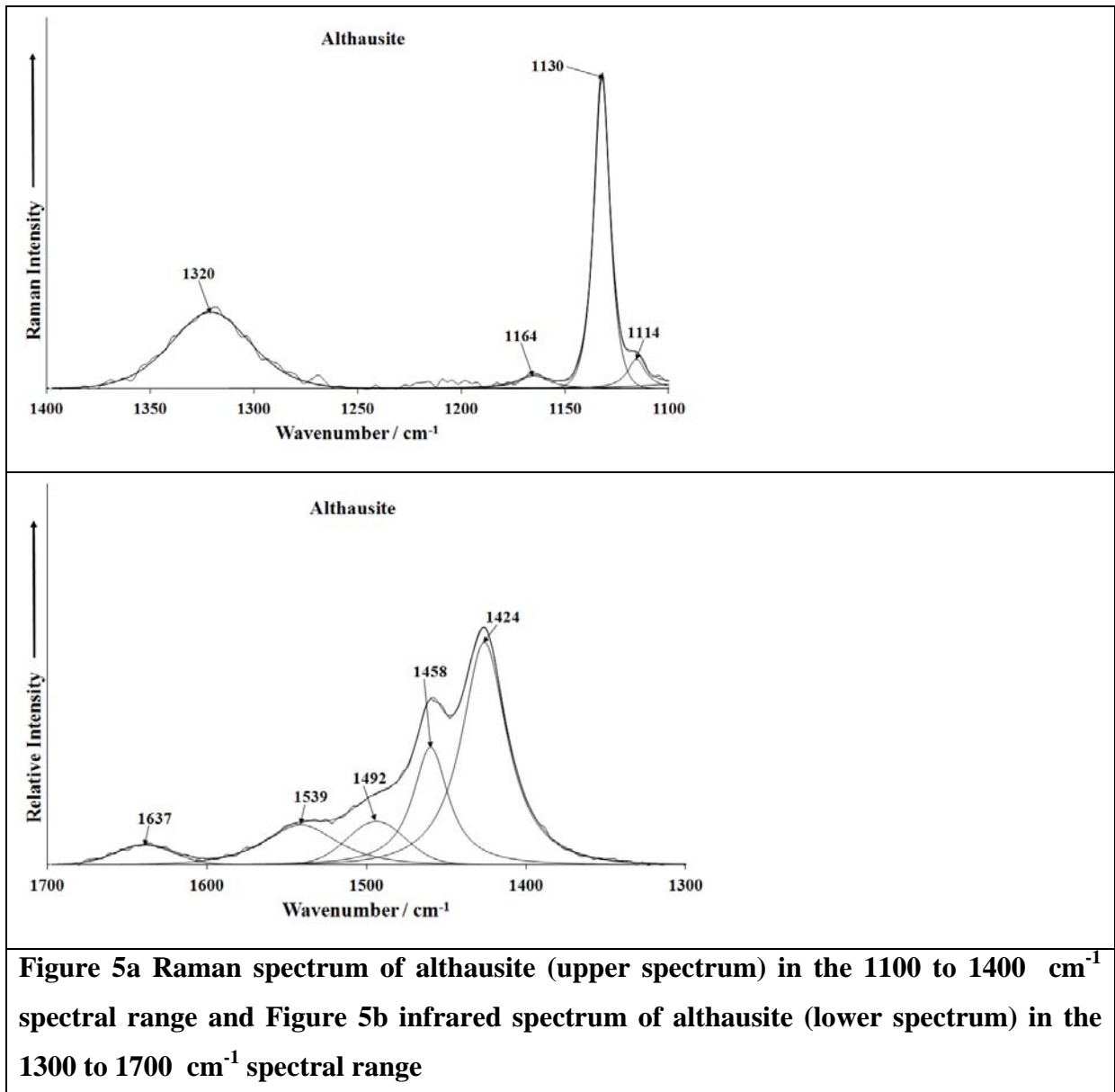


Figure 4a Raman spectrum of althausite (upper spectrum) in the 1900 to 2400  $\text{cm}^{-1}$  spectral range and Figure 4b infrared spectrum of althausite (lower spectrum) in the 2800 to 3500  $\text{cm}^{-1}$  spectral range





**Figure 5a Raman spectrum of althausite (upper spectrum) in the 1100 to 1400 cm<sup>-1</sup> spectral range and Figure 5b infrared spectrum of althausite (lower spectrum) in the 1300 to 1700 cm<sup>-1</sup> spectral range**

341

342

343

344

345